

Diamondoid hydrocarbons as a molecular proxy for thermal maturity and oil cracking: Geochemical models from hydrous pyrolysis

Zhibin Wei ^{a,*}, J. Michael Moldowan ^a, Shuichang Zhang ^b, Ronald Hill ^c,
Daniel M. Jarvie ^d, Huitong Wang ^b, Fuqing Song ^b, Fred Fago ^a

^a Department of Geological and Environmental Sciences, Stanford University, Stanford, CA 94305-2115, USA

^b Research Institute of Petroleum Exploration and Development, PetroChina, Beijing 100083, China

^c U.S. Geological Survey, Box 25046, Denver Federal Center, MS 939, Denver, CO 80225, USA

^d Humble Geochemical Services, Division of Humble Instruments & Services, Inc., P.O. Box 789, Humble, TX 77347, USA

Received 8 June 2006; received in revised form 19 September 2006; accepted 27 September 2006

Available online 11 December 2006

Abstract

A series of isothermal hydrous pyrolysis experiments was performed on immature sedimentary rocks and peats of different lithology and organic source input to explore the generation of diamondoids during the thermal maturation of sediments. Oil generation curves indicate that peak oil yields occur between 340 and 360 °C, followed by intense oil cracking in different samples. The biomarker maturity parameters appear to be insensitive to thermal maturation as most of the isomerization ratios of molecular biomarkers in the pyrolysates have reached their equilibrium values. Diamondoids are absent from immature peat extracts, but exist in immature sedimentary rocks in various amounts. This implies that they are not products of biosynthesis and that they may be generated during diagenesis, not just catagenesis and cracking. Most importantly, the concentrations of diamondoids are observed to increase with thermal stress, suggesting that they can be used as a molecular proxy for thermal maturity of source rocks and crude oils. Their abundance is most sensitive to thermal exposure above temperatures of 360–370 °C ($R_0 = 1.3$ – 1.5%) for the studied samples, which corresponds to the onset of intense cracking of other less stable components. Below these temperatures, diamondoids increase gradually due to competing processes of generation and dilution. Calibrations were developed between their concentrations and measured vitrinite reflectance through hydrous pyrolysis maturation of different types of rocks and peats. The geochemical models obtained from these methods may provide an alternative approach for determining thermal maturity of source rocks and crude oils, particularly in mature to highly mature Paleozoic carbonates. In addition, the extent of oil cracking was quantified using the concentrations of diamondoids in hydrous pyrolysates of rocks and peats, verifying that these hydrocarbons are valuable indicators of oil cracking in nature.

© 2006 Elsevier Ltd. All rights reserved.

1. Introduction

Thermally altered petroleum hydrocarbons, which include light oil, condensate and gas, represent

* Corresponding author. Tel.: +1 650 723 9057; fax: +1 650 723 8489.

E-mail address: weizb@stanford.edu (Z. Wei).

significant potential resources in deep subsurface reservoirs. With exploration targets pushing to ever increasing depth, it is essential to improve our understanding of the evolution of such light fluids by determining their thermal maturity and sources.

Various biomarker ratios based on thermally driven isomerizations at asymmetric carbons and side chain positions have been used to assess the thermal maturity of petroleum (e.g., Albrecht et al., 1976; Seifert and Moldowan, 1980; Mackenzie et al., 1980; Wei et al., 2001). However, because the abundance of biomarkers in expelled oils decreases rapidly with increasing thermal maturity, information provided from them at or after the peak generative stage in the oil window is limited and they provide little insight into the thermal history of highly mature oils and condensates (Peters et al., 2005).

Petroleum from multiple sources may charge a reservoir over geologic time, resulting in a mixture of hydrocarbons generated and expelled at varying degrees of thermal maturity. Because biomarkers from lower maturity sources dominate, source information from higher maturity oils and condensates is likely to be overlooked. Molecular and isotopic compositions of light hydrocarbons and gas can provide information on higher maturity sources (e.g., Thompson, 1983; Hunt et al., 1980; Chung et al., 1998). Of these compounds, diamondoids appear to provide reliable information about high maturity fluids. Unlike biomarkers, they are thermally very stable due to their unique diamond-like cage structure. As a result, they remain in oils and condensates over geological time at elevated subsurface temperatures and pressures after all saturated biomarkers are destroyed. Dahl et al. (1999) proposed a diamondoid biomarker method based on their concentrations to determine thermal maturity for any oil and condensate samples at any maturity level. The method has proved to be a useful tool in estimating the thermal maturity of both oils and high maturity condensates and can be used in the recognition of the oil deadline, the calibration of expulsion efficiency models and the identification of mixed sources (Dahl et al., 1998).

Although the approach has been applied to improve our understanding of complex petroleum systems, little work has been done to elucidate the fundamental origins of diamondoids in source rocks. In this study, we use hydrous pyrolysis experiments to simulate and quantify the generation and

cracking of diamondoids and biomarkers from different immature source types. The objectives were: (1) to investigate how concentrations of different diamondoids change through generation and cracking; (2) to calibrate their concentrations with measured vitrinite reflectance (R_0) as a potential molecular proxy for thermal maturity; (3) to evaluate the utility of specific biomarker and diamondoid maturity ratios through generation and cracking of pyrolysates; (4) to determine the extent of oil cracking during hydrous pyrolysis of immature rocks and peats using the concentrations of diamondoids generated.

2. Samples and methods

2.1. Samples

The geochemical data for the rock and peat samples used are listed in Table 1. Samples #24, an immature Permian limestone with total organic carbon (TOC) = 2.4 wt%, and #27, an immature oil shale, were collected from the Irati Formation, Southern Brazil. The Nevada sample # V19.13 is an immature Ordovician carbonate from the Vinini Creek Formation. Fen and bog peats from Germany are representative sources dominated by higher land plant input. These immature peat samples have TOC values > 34% and vary in their hydrogen index (HI) and production index (PI) values.

2.2. Hydrous pyrolysis of immature rocks and peats

The rocks were ground to 0.5–2 cm chunks. The chunks (ca. 30 g) and peats (ca. 10 g) were loaded into T-316 stainless steel vessels to which 15 mL of distilled water was added to submerge the rocks. The vessels then were flushed with Ar for 1 min before sealing, placed into a furnace and heated isothermally for 72 h in a series of experiments with increasing temperature from 230 up to 450 °C. After reaction, the reactors were cooled, and the generated oil floating on the water surface and free oil sticking to the rock chips and inner walls were recovered by washing with $\text{CH}_2\text{Cl}_2:\text{CH}_3\text{OH}$. The washing solvents were removed using rotary evaporation. The removal of water and methanol was achieved using the funnel separatory method described by Wei et al. (2007) and anhydrous Na_2SO_4 was added to remove any residual water from pyrolysates. The solvents were evaporated

Table 1
Bulk data for rock and peat samples used in hydrous pyrolysis experiments

Sample	Lithology	Location	Formation	Age	R ₀ (%)	TOC (wt%)	T _{max} (°C)	S ₁ (mg/g)	S ₂ (mg/g)	S ₃ (mg/g)	S ₁ + S ₂ (mg/g)	PI	HI (mg HC/g TOC)	OI (mg CO ₂ /g TOC)	Type of organic matter
#24	Limestone	Southern Brazil	Irati	Permian	0.43	2.40	430	4.70	17.78	0.43	22.48	0.21	741	18	I
#27	Shale	Southern Brazil	Irati	Permian	0.45	6.96	422	6.30	33.37	0.77	39.67	0.16	479	11	I
#V19.13	Limestone	Nevada	Vinini Creek	Ordovician	0.51	1.74	433	0.65	8.58	0.38	9.23	0.07	493	22	II
#34	Fen peat	Germany	Outcrop		0.20	37.88	401	24.11	59.74	35.94	83.85	0.29	158	95	III
#35	Bog peat	Germany	Outcrop		0.20	34.38	403	50.66	35.40	34.96	86.06	0.59	103	102	III

under a N₂ flow at room temperature to minimize loss of volatile adamantanes.

2.3. Rock-Eval pyrolysis and X-ray diffraction (XRD)

Rock-Eval pyrolysis provides bulk information about the model rocks and peats such as the abundance of organic matter, maturity and hydrocarbon generative potential. Measurements were made using a Rock-Eval II Plus TOC instrument under standard conditions (heating from 300 to 600 °C at 25 °C/min under He flow).

XRD analysis was carried out to determine the mineralogical composition of the immature source rocks used in the hydrous pyrolysis experiments. Measurements were made using a Siemens D500 X-ray diffraction system run at 40 kilovolts (kV) and 30 milliamperes (mA). Samples were prepared by grinding rock chips in a ball mill until powdered (< 40 μm). ZnO standard (0.111 g) was added to each powdered rock sample (1.000 g), which was then ground in a McCrone mill for 5 min with CH₃OH (4 mL). Samples were dried, sieved and side packed into a holder to ensure random orientation. They were X-rayed from 5° to 65° 2θ using Cu Kα radiation at 0.02° steps and a count time of 2 s per step. The computer program RockJock estimated mineral abundances, including clay minerals (e.g., kaolinite, Ca-smectite, 1 M illite) and non-clays (e.g., feldspar, calcite, dolomite, pyrite) from the X-ray diffraction data. Details of the methods used to prepare samples and determine quantitative mineral amounts are described by Eberl (2003).

2.4. Vitrinite reflectance

Vitrinite reflectance was measured on the reacted rock and peat samples. Inorganic minerals were removed from the whole rock using HCl and HF and the kerogen was concentrated further by flotation in a ZnBr₂ solution. Isolated kerogen was mixed with epoxy, mounted in an acrylic plug and polished using progressively finer grades of silicon carbide and finally polished with water-based alumina suspensions prior to taking reflectance readings using a Zeiss Universal microscope and photomultiplier. The indigenous population was assigned to the telocollinite maceral of vitrinite. The color of palynomorphs, recorded as thermal alternation index (TAI), was determined on kerogen

strew mounts and found to complement the vitrinite reflectance values.

2.5. Ultrasonic extraction

The rocks and peats were extracted ultrasonically with $\text{CH}_2\text{Cl}_2:\text{CH}_3\text{OH}$ (1:1 v:v) for 24 h. The extracts were decanted to a 125 mL separatory funnel containing deionized water. The aqueous bottom layer was separated, extracted ($\times 3$) with pentane: CH_2Cl_2 (2:1 v:v). The combined extracts were treated with anhydrous sodium sulfate to remove residual water. The solvents were evaporated carefully under a nitrogen flow to minimize loss of volatile hydrocarbons. The details are described by Wei et al. (2007).

2.6. Gas chromatography-flame ionization detection (GC-FID)

The toluene-diluted (100 \times) extracts of rock and peat samples and pyrolysates were analyzed using a Hewlett Packard 5890 GC equipped with a 100% methylsilicone DB-1 capillary column (24 m \times 0.2 mm i.d., film thickness 0.33 μm). H_2 served as carrier gas at a fixed 20 psi head pressure. Samples were injected at 80 $^\circ\text{C}$ and the oven was programmed at 10 $^\circ\text{C}/\text{min}$ to 320 $^\circ\text{C}$ where it was held for 15 min.

2.7. Liquid chromatography and branched and cyclic (B/C) separation

The extracts and hydrous pyrolysates were spiked with deuterated diamondoids and 5 β -cholane for quantification of diamondoids, C_{29} $\alpha\alpha\alpha$ stigmastane 20R and C_{30} 17 α -hopane. The deuterated diamondoid internal standards were synthesized in the Molecular Organic Geochemistry Laboratory at Stanford University and include D_4 -adamantane, D_3 -1-methyladamantane, D_3 -1-methyldiamantane, D_4 -diamantane, D_5 -ethyldiamantane and D_4 -triamantane. The extracts and pyrolysates were fractionated using silica gel column chromatography with hexane and CH_2Cl_2 to obtain the saturate and aromatic fractions, respectively.

The B/C fraction was obtained by the removal of *n*-alkanes from the saturate fraction using ZSM-12 molecular zeolite with a pore size of 6 Å (Aldrich Chemical Company). The fraction was diluted with 20 parts toluene.

2.8. Selective ion recording-gas chromatography mass spectrometry (SIR-GC-MS)

SIR-GC-MS analysis was performed on the saturated hydrocarbon fractions using a Hewlett-Packard 5890 Series II Gas Chromatograph interfaced to a Fisons Instruments Autospec-Q Hybrid Mass Spectrometer. The GC was equipped with a 60 m J&W fused silica DB-1 capillary column (0.25 mm i.d.; 0.25 μm phase thickness of 100% methylsilicone). H_2 was used as carrier gas at a constant pressure of 15 psi. The temperature program was 50 $^\circ\text{C}$ for 2 min, 50–80 $^\circ\text{C}$ at 15 $^\circ\text{C}/\text{min}$, 80–290 $^\circ\text{C}$ at 2.5 $^\circ\text{C}/\text{min}$, 290–320 $^\circ\text{C}$ at 25 $^\circ\text{C}/\text{min}$ and 320 $^\circ\text{C}$ for 25 min. The injection port and transfer line temperature was 325 $^\circ\text{C}$.

The following ions were monitored for diamondoid analysis: m/z 135, 136, 140, 149, 187, 188, 192, 201, 239, 240 and 244. Quantification of adamantanes, diamantanes and triamantanes was achieved by integration of peak heights with respect to the corresponding standards, D_3 -1-methyladamantane, D_3 -1-methyldiamantane, and D_4 -triamantane, respectively. The quantitation of tetramantanes was made relative to the D_4 -triamantane standard and D_5 -1-ethyldiamantane was used to quantify ethyldiamantanes. The quantitation of C_{29} $\alpha\alpha\alpha$ stigmastane 20R was achieved by comparing the corresponding area with that of 5 β -cholane using m/z 217 in SIR-GCMS analysis. Hopanes were analyzed by monitoring m/z 191. Duplicate experiments indicated that the standard deviation was typically < 8% for the diamondoid and biomarker measurements.

2.9. Metastable reaction monitoring-gas chromatography mass spectrometry (MRM-GC-MS)

The toluene-diluted B/C fractions were analyzed using the GC-MS system described above in the MRM mode. Splitless injection of B/C fractions (1 μL) was made and the temperature program was isothermal at 80 $^\circ\text{C}$ for 1 min, then at 2 $^\circ\text{C}/\text{min}$ to 320 $^\circ\text{C}$ where it was held for 20 min. The mass spectrometer was run in parent \rightarrow daughter mode for sterane analysis. The monitored transitions were: m/z 330 \rightarrow 217, 358 \rightarrow 217, 372 \rightarrow 217, 386 \rightarrow 217, 400 \rightarrow 217, 414 \rightarrow 217, and 414 \rightarrow 231. Dwell time was 50 ms for each transition with a 70 ms interchannel delay. Ionization energy was 70 eV.

3. Results and discussion

3.1. Bulk geochemistry of immature rocks and peats

The initial rocks and peat samples were thermally immature as indicated by their measured R_0 values and Rock-Eval T_{\max} values (Table 1). Rock-Eval pyrolysis data also show that the T_{\max} values of the Irati rocks are below 435 °C, which is considered the threshold for the oil window (Tissot and Welte, 1984). The HI values of the Irati limestone and oil shale are 741 and 479 mg HC/g TOC, and oxygen indices (OI) are 18 and 11 mg CO₂/g TOC, consistent with a dominance of oil prone Type I organic matter (Fig. 1). The Vinini limestone is likely dominated by Type II organic matter. The bog and fen peats have very low T_{\max} and HI values (Table 1). Both organic-rich modern sediments are gas prone and dominated by type III organic matter, as illustrated in Fig. 1.

3.2. Thermal maturity, organic matter input and depositional environment

The 22S/(22S + 22R) isomerization ratios for C₃₂ 17 α -homohopane are < 0.58 for Irati oil shale and limestone and German peats. Other biomarker parameters, such as 20S/(20S + 20R), $\beta\beta/(\alpha\alpha + \beta\beta)$, dia/(dia + reg)-steranes, Ts/(Ts + Tm), $\beta\alpha/(\beta\alpha + \alpha\beta)$ -hopanes, and tricyclics/(tricyclics + 17 α -hopanes) also indicate that these samples are immature

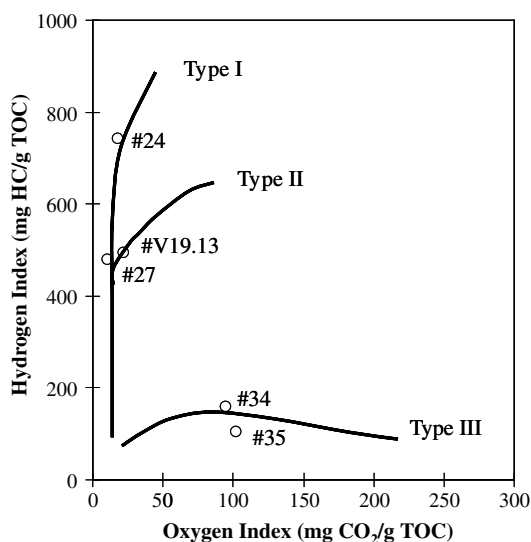


Fig. 1. Hydrogen index versus oxygen index diagram showing type of organic matter in the immature rocks and peats. Data obtained from Rock-Eval pyrolysis.

(Table 2). Although the 22S/(22S + 22R) and 20S/(20S + 20R) ratios reach the equilibrium values in the Nevada carbonate (Table 2), such values have been reported in marginally mature source rocks (e.g., Schoell et al., 1983). Tric/(tric + 17 α -hops) and Ts/(Ts + Tm) ratios also are relatively low, consistent with the Nevada carbonate sample being marginally mature.

It has been suggested that the C₂₉ steranes derive from a land plant source, while C₂₇ steranes are sourced from marine algae (e.g., Czochanska et al., 1988). If true, the Irati limestone and oil shale and Vinini limestone would be considered to be dominated by organic matter input from terrestrial higher plants. However, algal source input may also contribute to a high relative abundance of C₂₉ steranes (Volkman, 1986). The positive correlation between C₂₉ and C₃₀ steranes (24-*n*-propylcholestanes) in Irati samples, the latter of which is derived exclusively from marine algae (Moldowan et al., 1990), reflects the predominance of marine algal input for the oil shale and limestones during deposition. Oleanane is not detectable in the Irati samples or Vinini limestone. In contrast, oleanane/C₃₀ hopane ratios are very high in the peat samples, especially in bog peat, consistent with both peats being dominated by higher plant input.

The regular stair-step progression of C₃₁–C₃₅ homohopanes is consistent with sub-oxic bottom waters during deposition for these rocks and peats. The high gammacerane index of the Irati limestone indicates highly reducing, hypersaline conditions during deposition (Moldowan et al., 1985; Fu et al., 1986). This limestone is an intercalated deposit within the shale body and the relatively high abundance of gammacerane in Irati oil shale suggests that the depositional environment of the shale is similar to that of the limestone. However, the very low gammacerane indices in Vinini carbonate and German fen peat suggest a sub-oxic environment. Pr/Ph value for the Vinini limestone indicates that it might be more reducing.

C₃₀^{*}/C₂₉ Ts ratios indicate that Germany fen peat, Irati oil shale and Vinini limestone were deposited in oxic to sub-oxic and clay-rich depositional environments. Alternatively, the relatively high C₃₀^{*}/C₂₉ Ts ratio for Vinini limestone might be attributed to its higher maturity. The formation of 17 α -diahopane is likely clay dependent (Moldowan et al., 1991; Wei et al., 2007) and so its absence from the Irati limestone and the German bog peat may be due to the absence of clay.

Table 2
Biomarker parameters for saturate fraction from extracts of unheated rocks and peats

Biomarker parameter	#24	#27	#V19.13	#34	#35
C ₂₇ :C ₂₈ :C ₂₉ Steranes	25:19:56	30:20:50	36:7:57	28:26:46	30:28:42
C ₂₇ :C ₂₈ :C ₂₉ Diasteranes	28:16:56	45:20:35	24:10:66	34:32:34	41:27:32
C ₃₀ /(C ₂₇ -C ₃₀) Steranes	0.023	0.019	0.048	0.008	0.011
ββ/(αα + ββ) ^a	0.30	0.21	0.57	0.49	0.33
C ₂₉ ααα 20S/(20S + 20R)	0.38	0.16	0.52	0.50	0.38
Dia/(dia + reg)-steranes ^b	0.33	0.09	0.17	0.42	0.35
C ₂₉ βα 20S/(20S + 20R)	0.50	0.52	0.62	0.53	0.43
22S/(22S + 22R) ^c	0.34	0.45	0.58	0.54	0.24
Ts/(Ts + Tm)	0.38	0.17	0.11	0.17	0.06
Oleanane/C ₃₀ hopane				0.13	1.98
Gammacerane/C ₃₀ hopane	28.55	0.55	0.05	0.16	
Tric/(tric+17α-hops) ^d	0.24	0.03	0.07	0.13	0.001
βα/(βα + αβ)-hopanes	0.69	0.14	0.07	3.25	2.27
C ₃₁ /(C ₃₁ -C ₃₅) Hops ^e	0.37	0.59	0.42	0.82	1.00
C ₃₂ /(C ₃₁ -C ₃₅) Hops	0.38	0.22	0.28	0.08	
C ₃₃ /(C ₃₁ -C ₃₅) Hops	0.15	0.10	0.14	0.09	
C ₃₄ /(C ₃₁ -C ₃₅) Hops	0.06	0.06	0.10	0.01	
C ₃₅ /(C ₃₁ -C ₃₅) Hops	0.04	0.03	0.06		
C ₃₀ [*] /C ₂₉ Ts ^f		0.14	0.13	0.23	

^a ββ/(αα + ββ) = C₂₉ regular steranes ββ/(αα + ββ).

^b Dia/(dia + reg)-steranes = Diasteranes/(diasteranes + regular steranes).

^c 22S/(22S + 22R) = C₃₂ Homohopane 22S/(22S + 22R).

^d Tric/(tric+17α-hops) = tricyclics/(tricyclics+17α-hopanes).

^e C₃₁/(C₃₁-C₃₅) Hops = C₃₁/(C₃₁-C₃₅) Homohopanes.

^f C₃₀^{*}/C₂₉ Ts = 17α-Diahopane/18α-30-norneohopane.

3.3. Oil generation from immature rocks and peats during hydrous pyrolysis

Non-gaseous, hydrous pyrolysate products include oil floating on water plus oil washed by solvent from occlusion on the sides of the pyrolysis vessel and rock surfaces. The pyrolysate yield is expressed as grams of recovered pyrolysate per gram of rock and/or peat. Fig. 2 shows the quantitative generation curves for pyrolysates from the rocks and peats with increasing reaction temperature following hydrous pyrolysis for 72 h. As pyrolysis temperature increases, oil is progressively generated.

As shown in Fig. 2, the yield of pyrolysate increases rapidly and maximizes at 340 °C for the bog and fen peats, at 350 °C for Irati oil shale and at 360 °C for the limestones, as the kerogen produces increasing amounts of liquid hydrocarbons through progressive evolution. A progressive decrease in pyrolysate yield is observed above those temperatures, which is indicative of thermal cracking of generated oil to pyrobitumen and gas (Lewan, 1993). Rock mineralogy may contribute

to the differences in the oil generation profiles. The Irati oil shale contains a higher content of clay minerals than the Irati and Vinini limestones (Table 3). Upon thermal stress, clay minerals are expected to absorb the organic molecules produced in oil generation and thereby catalyze both the thermal decomposition of kerogen to form oil and gas and the thermal cracking reaction of oil in nature (Tannenbaum and Kaplan, 1985; Huizinga et al., 1987a, 1987b). Thus, the presence of clay minerals could lead to the early occurrence of oil cracking and kerogen degradation (Tannenbaum and Kaplan, 1985; Hill et al., personal communication).

3.4. Molecular biomarkers and related maturity parameters

Various maturity parameters, including concentrations of C₃₀ 17α-hopane and C₂₉ ααα stigmastane 20R, and biomarker ratios for hydrous pyrolysates, are summarized in Table 4. These data were obtained from SIR-GC-MS analysis of the pyrolysates. The distributions of terpanes and steranes

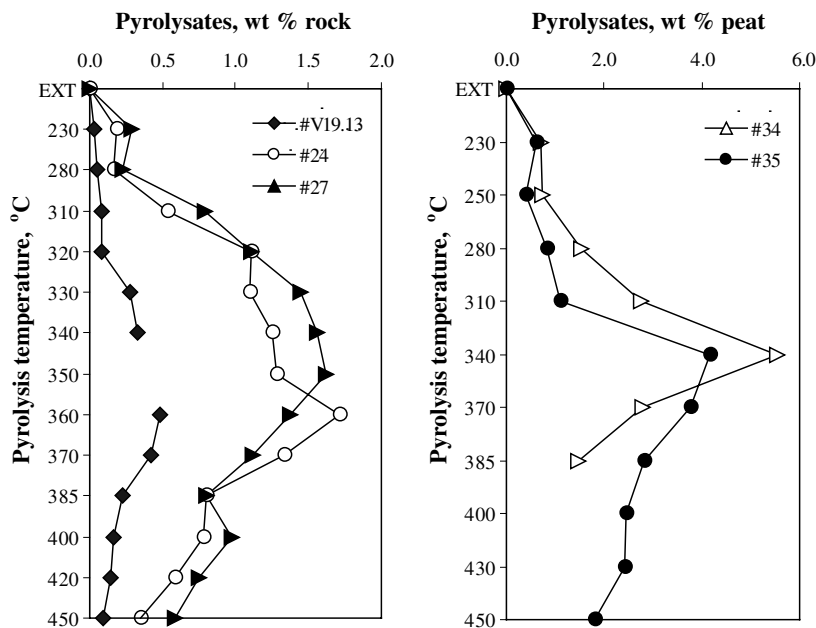


Fig. 2. Hydrous pyrolysate yield from immature rocks and peats vs. increasing temperature during hydrous pyrolysis of immature rocks and peats. EXT = extract yield prior to pyrolysis.

Table 3
Mineral composition^a of rock samples used in hydrous pyrolysis experiments

Composition		#24	#27	#V19.13
Non-clays	Quartz	30.8	37.8	12.2
	Feldspar	3.0	17.0	
	Calcite	0.8	6.7	50.3
	Dolomite	53.6	3.2	29.6
	Pyrite	0.2	3.3	
	Other non-clays	6.0	1.1	
Clays	Kaolinite	1.1	1.5	
	Ca-smectite	3.7	10.4	7.9
	1M illite	0.7	9.1	
	Other clays		9.9	

^a Estimated using RockJock.

change remarkably with increasing thermal maturity during hydrous pyrolysis of Vinini limestone (Figs. 3 and 4). The abundance of tricyclic terpanes increases significantly compared with that of 17 α -hopanes at 340 °C (Fig. 3). It is known that C₃₀ 17 α -hopane in sedimentary rocks is derived from bacterial membrane lipids (Ourisson et al., 1982). Upon thermal stress, this compound is generated either from functionalized triterpenols in immature rocks or from thermal decomposition of the kerogen skeleton. Fig. 5 shows that the concentration of C₃₀ 17 α -hopane maximizes at about 80 ppm at

230 °C in Vinini limestone. However, the highest concentration occurs at much higher temperature for the other immature rocks and peats (Fig. 5). This might be due to differences in either source input or thermal maturity between the Vinini limestone and other samples. The generation profile of C₂₉ $\alpha\alpha\alpha$ stigmasterane shows that sterane release generally occurs much earlier than that of hopanes (Fig. 5). This may be due to the fact that steranes are bound to the kerogen matrix via one linkage, while hopane precursors may have multiple linkages. At higher temperature, the concentrations of C₃₀ 17 α -hopane and C₂₉ $\alpha\alpha\alpha$ stigmasterane decrease dramatically due to chemical rearrangements and thermal cracking to smaller molecules. In addition, C₂₁ pregnanes and C₂₂ methyl pregnanes become more abundant with increasing thermal maturity, probably due to thermal breakdown of high molecular weight steranes (Fig. 4). As illustrated in Figs. 3 and 4, both biomarkers are virtually absent from pyrolysates above 400 °C because they are some of the least thermally stable saturated hydrocarbon species in petroleum and are subject to intense cracking. It is also noteworthy that sterane generation is already significantly reduced in the range of temperature corresponding to peak pyrolysate yield.

The Pr/Ph ratio generally tends to increase with maturity (Connan, 1974). Our results show that

Table 4
Biomarkers generated from hydrous pyrolysis of immature rocks and peats and molecular maturity parameters^a

Sample	T (°C)	A	B	C	D	E	F	G	H	I	J
#24	Unheated	1.36	0.33	0.38	0.54	0.38	0.38	0.30	0.44	42.05	3.83
	230	1.59	0.21	0.50	0.86	0.18	0.46	0.30	0.15	38.30	5.21
	280	1.35	0.40	0.41	0.82	0.25	0.43	0.33	0.17	50.15	6.10
	310	1.63	0.40	0.20	0.22	0.19	0.44	0.33	0.25	92.09	21.89
	320	2.11	0.47	0.17	0.15	0.32	0.43	0.29	0.36	105.78	33.51
	330	1.90	0.41	0.16	0.17	0.39	0.49	0.43	0.41	137.90	25.08
	340	2.72	0.53	0.11	0.13	0.41	0.44	0.38	0.39	57.28	36.05
	350	1.71	0.50	0.12	0.12	0.40	0.51	0.45	0.45	144.01	66.95
	360	2.00	0.55	0.14	0.18	0.45	0.43	0.38	0.37	37.90	40.19
	370	3.11	0.61	0.78	0.83	0.43	0.47	0.40	0.26	0.22	1.11
	385	1.15	0.61	0.73	0.74	0.52	0.57	0.51	0.51	0.01	0.76
	400	2.10	0.62	0.93	0.96	n.a.	n.a.	n.a.	n.a.	n.a.	0.32
	420	n.a.	n.a.	n.a.	n.a.	n.a.	n.a.	n.a.	n.a.	n.a.	n.a.
	450	n.a.	n.a.	n.a.	n.a.	n.a.	n.a.	n.a.	n.a.	n.a.	n.a.
#27	Unheated	1.25	0.45	0.17	0.06	0.16	0.16	0.21	0.07	1051.50	13.96
	230	1.26	0.43	0.19	0.06	0.15	0.20	0.19	0.06	1191.60	14.26
	280	1.40	0.42	0.12	0.04	0.16	0.24	0.22	0.11	1212.70	12.27
	310	2.17	0.48	0.06	0.03	0.20	0.25	0.24	0.07	213.71	42.80
	320	1.58	0.47	0.20	0.08	0.28	0.36	0.18	0.21	141.00	59.33
	330	1.49	0.42	0.21	0.08	0.30	0.41	0.21	0.16	246.89	52.77
	340	2.07	0.44	0.04	0.03	0.24	0.39	0.26	0.11	47.47	43.96
	350	1.92	0.53	0.25	0.14	0.38	0.45	0.35	0.20	60.51	51.70
	360	1.87	0.60	0.27	0.22	0.31	0.42	0.29	0.18	20.31	29.40
	370	1.70	0.46	0.06	0.04	0.23	0.33	0.25	0.12	1.79	3.23
	385	1.46	0.59	0.21	0.14	0.43	0.53	0.34	0.22	0.64	1.87
	400	2.34	0.43	0.11	0.11	0.22	0.47	0.26	0.11	0.03	1.51
	420	n.a.	n.a.	n.a.	n.a.	n.a.	n.a.	n.a.	n.a.	n.a.	n.a.
	450	n.a.	n.a.	n.a.	n.a.	n.a.	n.a.	n.a.	n.a.	n.a.	n.a.
#V19.13	Unheated	0.89	0.58	0.11	0.11	0.52	0.52	0.57	0.30	700.45	41.07
	230	1.19	0.60	0.29	0.12	0.51	0.59	0.54	0.38	718.70	79.78
	280	1.13	0.61	0.30	0.12	0.44	0.54	0.45	0.31	728.91	49.84
	310	1.12	0.60	0.17	0.08	0.55	0.58	0.56	0.40	487.32	47.97
	320	1.63	0.60	0.23	0.14	0.41	0.52	0.51	0.41	261.53	37.86
	330	1.98	0.61	0.19	0.11	0.47	0.50	0.49	0.32	170.97	28.52
	340	2.79	0.47	0.17	0.15	0.27	0.50	0.35	0.21	84.75	21.29
	360	0.78	0.61	0.30	0.22	0.50	0.54	0.54	0.44	27.72	43.32
	370	1.95	0.61	0.26	0.11	0.53	0.59	0.56	0.38	1.50	3.30
	385	1.17	0.62	0.24	0.15	0.54	0.56	0.57	0.40	0.21	1.12
	400	1.42	0.60	0.61	0.11	0.51	0.57	0.53	0.37	0.10	0.89
	420	n.a.	n.a.	n.a.	n.a.	n.a.	n.a.	n.a.	n.a.	n.a.	n.a.
	450	n.a.	n.a.	n.a.	n.a.	n.a.	n.a.	n.a.	n.a.	n.a.	n.a.
	#34	Unheated	1.50	0.34	0.17	0.20	0.50	0.50	0.49	0.57	1.58
230		0.91	0.42	0.25	0.30	0.21	0.35	0.32	0.04	35.38	15.93
250		1.49	0.45	0.32	0.53	0.26	0.49	0.38	0.08	59.79	10.87
280		2.51	0.22	0.36	0.79	0.14	0.50	0.49	0.03	157.07	20.85
310		3.60	0.14	0.51	0.70	0.13	0.33	0.34	0.04	313.08	50.81
340		3.31	0.27	0.50	0.68	0.21	0.48	0.42	0.17	71.49	53.86
370		4.31	0.45	0.64	1.01	0.22	0.42	0.35	0.25	9.28	23.15
400		1.15	0.52	0.65	0.72	0.19	0.46	0.34	0.18	1.52	4.73
#35		Unheated	1.63	0.24	0.06	0.27	0.38	0.38	0.33	0.40	13.11
	230	1.12	0.33	0.43	0.39	0.13	0.31	0.19	0.03	190.45	18.18
	250	3.13	0.19	0.36	0.46	0.05	0.40	0.12	0.03	557.53	20.37
	280	2.83	0.21	0.47	0.89	0.06	0.47	0.22	0.07	124.80	27.30
	310	2.96	0.18	0.49	0.34	0.05	0.46	0.21	0.06	109.86	51.31

Table 4 (continued)

Sample	T (°C)	A	B	C	D	E	F	G	H	I	J
	340	4.62	0.25	0.37	0.43	0.08	0.50	0.16	0.07	93.08	32.12
	370	4.00	0.37	0.66	0.51	0.23	0.50	0.33	0.18	8.24	17.12
	385	1.28	0.45	0.61	0.42	0.32	0.51	0.34	0.17	0.50	10.21
	400	1.40	0.47	0.64	0.25	0.34	0.44	0.30	0.14	0.12	5.07
	430	n.a.	n.a.	n.a.	n.a.	n.a.	n.a.	n.a.	n.a.	n.a.	n.a.
	450	n.a.	n.a.	n.a.	n.a.	n.a.	n.a.	n.a.	n.a.	n.a.	n.a.

^a A = Pr/Ph; B = 22S/(22S + 22R) C₃₂ 17 α -hopane; C = Ts/(Ts + Tm); D = Ts/C₃₀ 17 α -hopane; E = 20S/(20S + 20R) C₂₉ 5 α ,14 α ,17 α -sterane; F = 20S/(20S + 20R), 13 β ,17 α -diasteranes; G = $\beta\beta$ /($\beta\beta$ + $\alpha\alpha$) C₂₉ steranes; H = diasteranes/regular steranes; I = ppm total C₂₉ $\alpha\alpha\alpha$ stigmastane 20R in pyrolysates; J = ppm total C₃₀ 17 α -hopane in pyrolysates; n.a. = not available.

the Pr/Ph ratio increases until 340 °C for the immature rocks and bog peat, and 370 °C for fen peat. Beyond that, a reversal in the ratio is generally

observed. This is in agreement with the results reported by Albrecht et al. (1976) and Radke et al. (1980). However, Pr/Ph ratios are not recommended

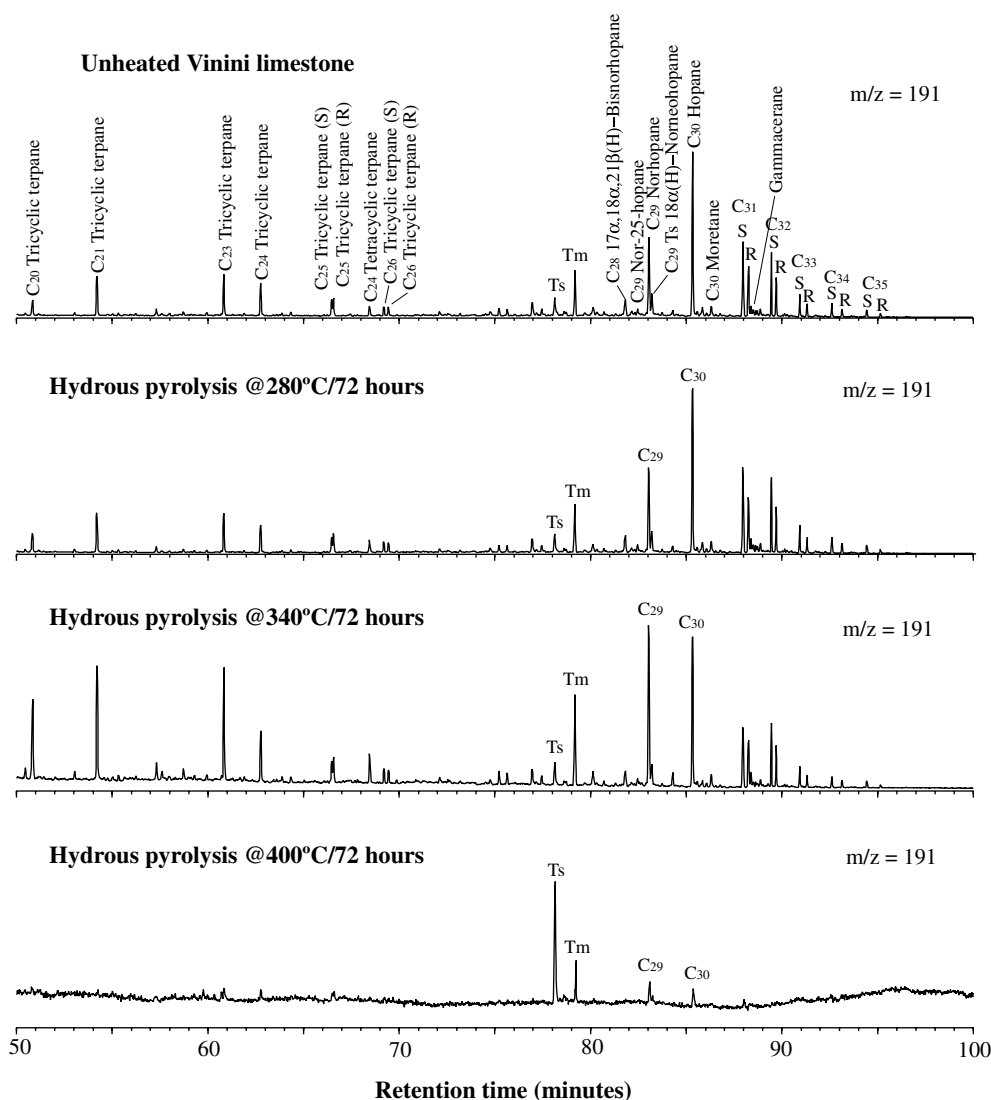


Fig. 3. Terpene mass chromatograms (m/z 191) for extract of unheated Vinini limestone and hydrous pyrolysates for 280, 340, and 400 °C, showing change in distribution with increasing thermal stress.

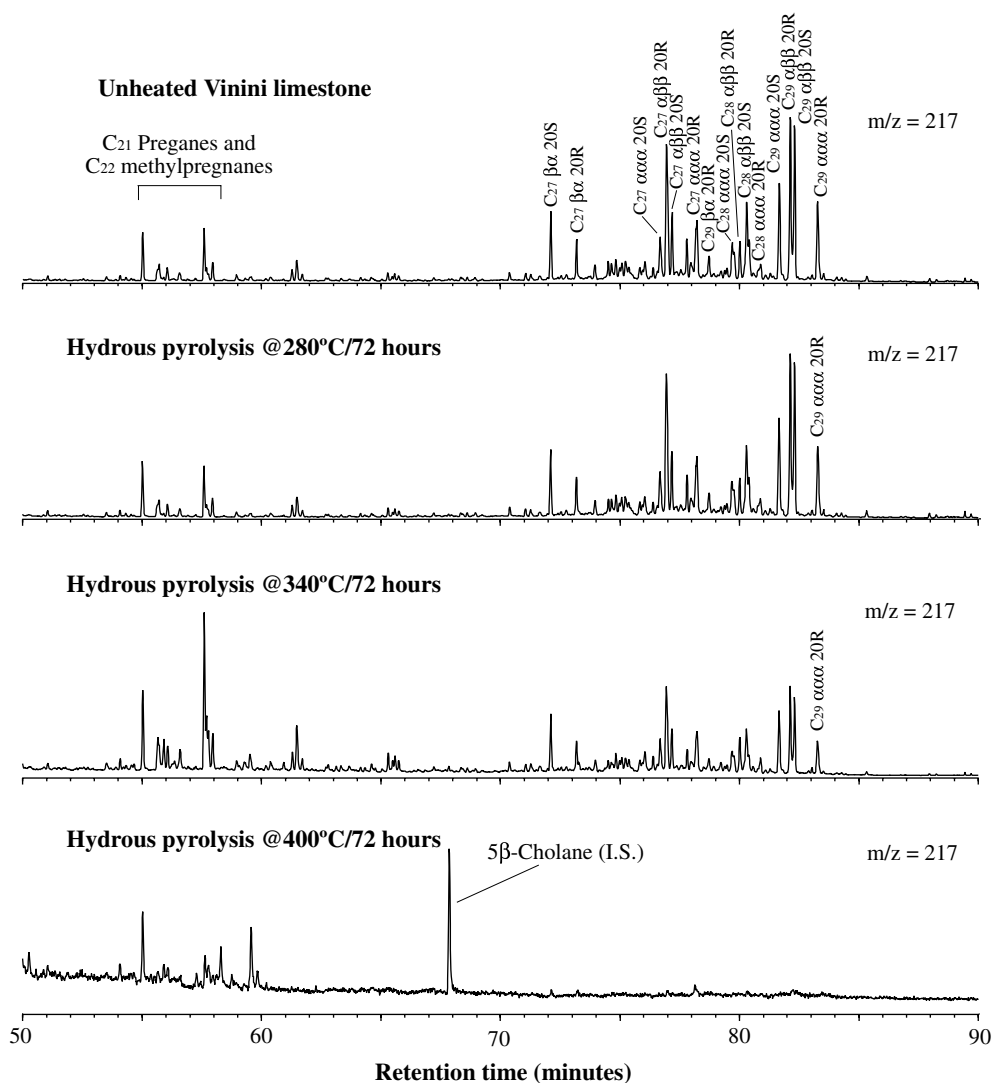


Fig. 4. Sterane mass chromatograms (m/z 217) for extract of unheated Vinini limestone and hydrous pyrolysates for 280, 340, and 400 °C, showing change in distribution with increasing thermal stress.

for assessment of thermal maturity since they are primarily influenced by source input. The hopane and sterane isomerization reactions generally reach equilibrium in the early oil window. This may result in constant values for isomerization-based ratios such as $22S/(22S + 22R)$ and $20S/(20S + 20R)$ with increasing maturity, which can be observed for the Vinini limestone (Table 4). However, the equilibrium between 20R (biological epimer) and 20S (geological epimer) seems to occur at higher temperature for the Irati limestone and oil shale. The ratio also changes unsystematically with increasing thermal stress.

$T_s/(T_s + T_m)$ and T_s/C_{30} 17α -hopane values appear to increase with increasing pyrolysis temper-

ature for Irati limestone and Germany bog and fen peats. Even so, the absence of these biomarkers from pyrolysates generated at higher maturity limits their application at higher maturity. Furthermore, both ratios exhibit large variations for Irati oil shale and Vinini limestone, which might be caused by the influence of organic facies. As shown in Table 4, the other sterane maturity parameters (e.g., $\beta\beta/(\alpha\alpha + \beta\beta)$, diasteranes/regular steranes) normally used for source rocks and crude oils do not show any trend with increasing maturity. The proposed $\beta\beta/(\alpha\alpha + \beta\beta)$ equilibrium values of ca. 0.67–0.71 (Seifert and Moldowan, 1980) are not reached for all the samples, even at extremely high maturity. Perhaps this is due to different mecha-

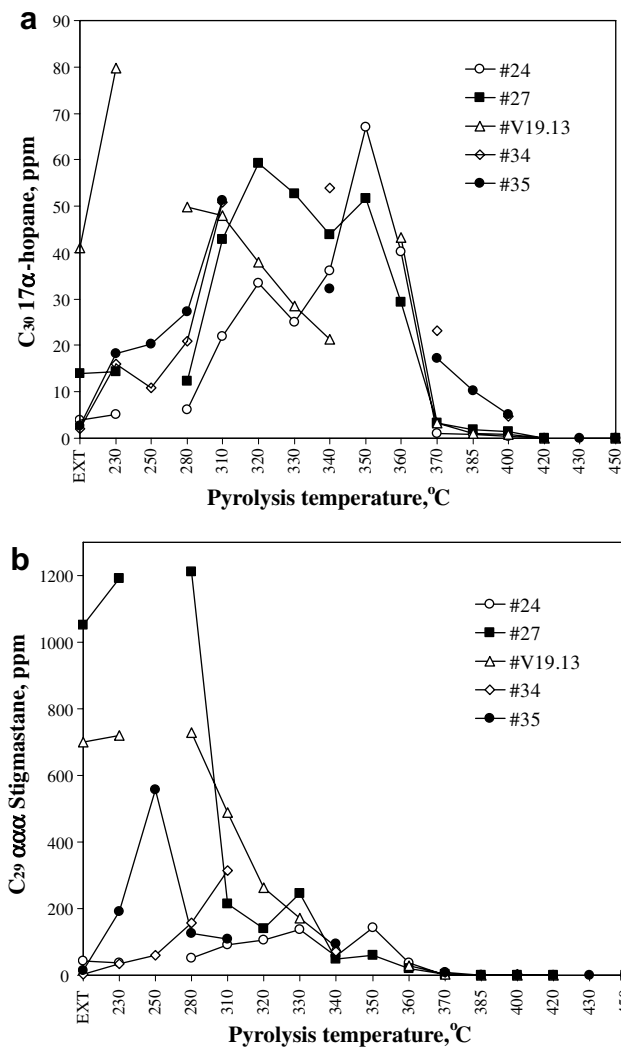


Fig. 5. Concentration of C₃₀ 17α-hopane and C₂₉ ααα stigmasterane 20R in hydrous pyrolysates from immature source rocks and peats for isothermal experiments at various temperatures. Concentrations were determined via SIR-GC-MS analysis and 5β-cholane standard quantitation. EXT = concentration in extract prior to pyrolysis.

nisms of epimerization at the high temperatures used in these experiments compared to more moderate temperatures experienced by rocks during natural maturation.

3.5. Mineralogy effects on diamondoid abundance in immature sedimentary rocks

The mass chromatograms for diamondoids are shown in Fig. 6 with peak identification in Table 5. Our results indicate that they are detectable in immature extracts of the Irati oil shale and limestone as well as Vinini limestone. The extracts of Vinini limestone contain relatively high abundances

(ca. 1.58 ppm). In comparison, the concentrations are much lower for both immature Irati rocks (Table 6). The existence of diamondoids in these immature rocks implies that they begin to form earlier than the beginning of oil generation.

It has been suggested that adamantanes are formed from the rearrangement of tricycloalkanes in the presence of Lewis acids (Petrov et al., 1974; Fort, 1976). In contrast, the occurrence of diamondoids in these immature sedimentary rocks may be attributable to molecular rearrangements of organic precursors during diagenesis as a result of lower temperature Brønsted acidity from the hydration of clay (Brown and Rhodes, 1997). Lewis acidity

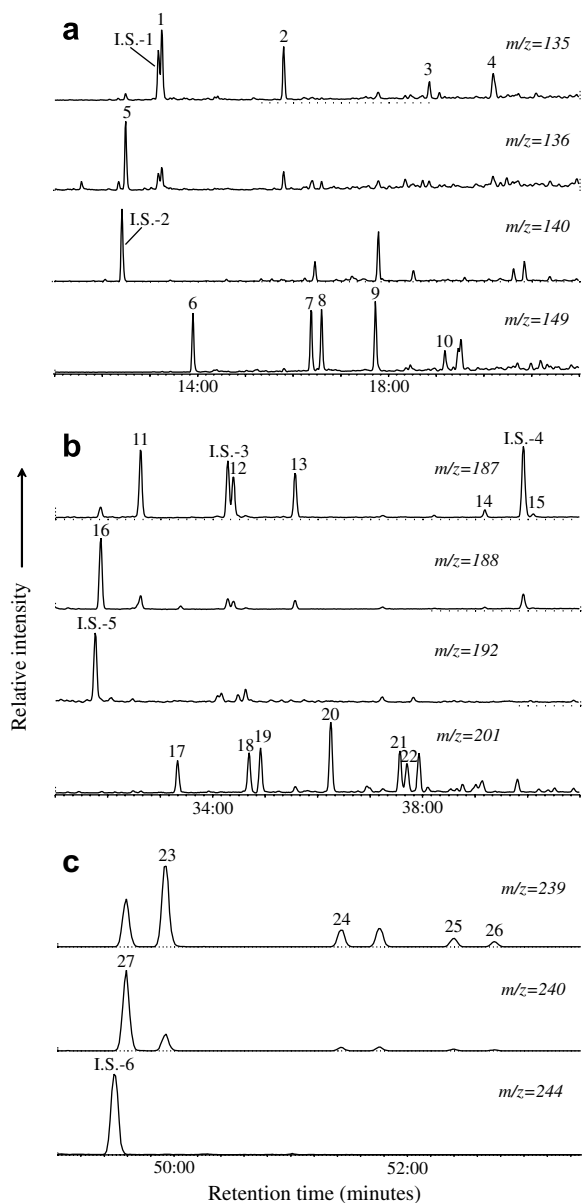


Fig. 6. Mass chromatograms of diamondoid hydrocarbons in hydrous pyrolysates from Irati oil shale at 400 °C, including (a) adamantanes, (b) diamantanes, (c) triamantanes determined via SIR-GC-MS. Peak identifications in Table 6.

predominates at higher temperatures, with the loss of water in the interlayer of clay (Cseri et al., 1995), which is favorable for the generation of diamondoids during catagenesis.

The concentration of diamondoids differs in the two Irati extracts, being twice as abundant in the oil shale than the limestone (Table 6). Rock mineralogy may be responsible for these differences. As previously demonstrated, CaCO_3 has a significant

inhibitive effect on the formation of diamondoids with maturation, whereas an increase in montmorillonite associated with kerogen leads to more diamondoids generated upon thermal stress (Wei et al., 2005a; Wei et al., 2006a). Thus, the higher abundance of dolomite and calcite (54%) and only trace amounts of Ca smectite (ca. 3.7%) and other clay minerals (ca. 2%) in the Irati limestone might lead to the lower concentrations of diamondoids (Table 3) in comparison to the Irati oil shale, which contains a much higher content of Ca smectite and other clay minerals.

Interestingly, the concentration of diamondoids in the extracts of the Vinini limestone with higher carbonate (ca. 79.9%) and approximately equivalent amounts of Ca smectite, are about four times higher than those in the Irati limestone extracts. This might be due to the difference in thermal stress experienced by these samples since diamondoid formation is maturity dependent (Wei et al., 2005b). As shown in Table 1, the Irati limestone is an immature rock ($R_0 = 0.43\%$), whereas the Vinini limestone is of marginal maturity ($R_0 = 0.51\%$). Therefore, higher quantities of diamondoids are expected to be generated from the Vinini limestone than the Irati limestone, as demonstrated by the hydrous pyrolysis experiments. Alternatively, the distinct chemical composition of extractable organic matter in these rocks might lead to the significant difference in the initial abundance of diamondoids in the samples. Wei et al. (2005b) suggested that, in the presence of suitable catalysts, a variety of organic compounds may yield diamondoids in varying amounts depending on their molecular nature. Isoprenoids and cycloalkanes are observed to generate greater amounts of diamondoids than other organic precursors (Wei, 2006b). Our analyses indicate that these organic compounds are more abundant in the marine Type II Vinini limestone than in the Irati limestone.

Diamondoid hydrocarbons are absent from the peat extracts (Table 6). Peat contains some aromatic hydroxy-, or methoxy-compounds, ketones and acids and is known to be a natural product of decaying plants, usually occurring under anaerobic and reducing conditions (Wollrab and Streibl, 1969; Tissot and Welte, 1984). Our peat has undergone only early diagenesis and the compounds are probably little altered from the original biosynthetic products. The absence of diamondoids from the extracts suggests that they are not biosynthetic products of higher plants.

Table 5
Peak identity from SIR-GC-MS analysis of saturate fraction from extracts and hydrous pyrolysates of rocks and peats

Peak no.	Molecular formula	Compound ^b	M ⁺ (<i>m/z</i>)	Base peak (<i>m/z</i>)
I.S.-1 ^a	C ₁₁ H ₁₅ D ₃	D ₃ 1-Methyladamantane	153	135
1	C ₁₁ H ₁₈	1-Methyladamantane	150	135
2	C ₁₁ H ₁₈	2-Methyladamantane	150	135
3	C ₁₂ H ₂₀	1-Ethyladamantane	164	135
4	C ₁₂ H ₂₀	2-Ethyladamantane	164	135
5	C ₁₀ H ₁₆	Adamantane	136	136
I.S.-2	C ₁₀ H ₁₂ D ₄	D ₄ Adamantane	140	140
6	C ₁₂ H ₂₀	1,3-Dimethyladamantane	164	149
7	C ₁₂ H ₂₀	1,4-Dimethyladamantane (<i>cis</i>)	164	149
8	C ₁₂ H ₂₀	1,4-Dimethyladamantane (<i>trans</i>)	164	149
9	C ₁₂ H ₂₀	1,2-Dimethyladamantane	164	149
10	C ₁₂ H ₂₀	2,6-+2,4-Dimethyladamantane	164	149
11	C ₁₅ H ₂₂	4-Methyldiamantane	202	187
I.S.-3	C ₁₅ H ₁₉ D ₃	D ₃ 1-Methyldiamantane	205	187
12	C ₁₅ H ₂₂	1-Methyldiamantane	202	187
13	C ₁₅ H ₂₂	3-Methyldiamantane	202	187
14	C ₁₆ H ₂₄	1-Ethyldiamantane	216	187
I.S.-4	C ₁₆ H ₁₉ D ₅	D ₅ 2-Ethyldiamantane	221	187
15	C ₁₆ H ₂₄	2-Ethyldiamantane	216	187
16	C ₁₄ H ₂₀	Diamantane	188	188
I.S.-5	C ₁₄ H ₁₆ D ₄	D ₄ Diamantane	192	192
17	C ₁₆ H ₂₄	4,9-Dimethyldiamantane	216	201
18	C ₁₆ H ₂₄	1,2-+2,4-Dimethyldiamantane	216	201
19	C ₁₆ H ₂₄	4,8-Dimethyldiamantane	216	201
20	C ₁₆ H ₂₄	3,4-Dimethyldiamantane	216	201
21	C ₁₆ H ₂₄	Dimethyldiamantane (1)	216	201
22	C ₁₆ H ₂₄	Dimethyldiamantane (2)	216	201
23	C ₁₉ H ₂₆	9-Methyltriamantane	254	239
24	C ₁₉ H ₂₆	5-Methyltriamantane	254	239
25	C ₁₉ H ₂₆	8-Triamantane	254	239
26	C ₁₉ H ₂₆	16-Triamantane	254	239
27	C ₁₈ H ₂₄	Triamantane	240	240
I.S.-6	C ₁₈ H ₂₀ D ₄	D ₄ Triamantane	244	244

^a Internal standard.

^b Structures and nomenclature are given in Appendix A.

3.6. Generation of diamondoids from thermal maturation of immature rocks and peats

Our results show that around 1 ppm of diamondoids is produced from the Irati type I source rocks prior to maximum yield temperature (and onset of oil cracking; Table 6). Hydrous pyrolysis of Vinini type II source rock produces up to about 5 ppm. The peats, representing Type III gas prone source rocks, generate an even lower abundance than the Type I and II rocks. In general, increasing pyrolysis temperature may enhance the strength of Lewis acidity of acidic clay minerals, causing more diamondoids to be formed and released into pyrolysates. However, the experiments show that, as the heating temperature increases, the abundance of diamondoids increases only slightly up through

peak yield (Table 6). The reason is that, although generation of diamondoids becomes more intense, substantial amounts of other hydrocarbons (e.g., *n*-alkanes, steranes, terpanes) are simultaneously formed through direct release from thermal degradation of kerogen or transformation from their unstable functionalized precursors (e.g., fatty acids, steroids, triterpenoids). These products dilute diamondoid abundances generated from kerogen, but also provide precursors for later production of diamondoids via molecular rearrangement in the presence of acidic clay minerals such as the Ca smectite in these rocks. The net effect of the maturation process is that diamondoids are both formed and diluted by other hydrocarbons within the oil window, resulting in relatively minor changes and variations in their concentration in the pyrolysates. As

Table 6
Diamondoids generated from hydrous pyrolysis of rocks and peats and derived maturity parameters

Sample ID	<i>T</i> (°C)	<i>R</i> ₀ (%)	Diamonoids ^a	Adam ^b	Diam ^c	Triam ^d	MDI ^e	MAI ^f	EAI ^g	DMAI ^h	DMDI-1 ⁱ	DMDI-2 ^j	MTI ^k
#24	Unheated	0.43	0.34	0.20	0.26	0.33	0.37	0.46	0.57	0.27	0.36	0.31	0.08
	230	0.56	0.36	0.98	0.37	0.56	0.26	0.44	0.33	0.26	0.31	0.23	0.15
	280	0.73	0.76	0.38	0.47	0.32	0.33	0.38	0.37	0.20	0.34	0.31	0.17
	310	0.94	0.52	0.42	0.30	0.49	0.31	0.34	0.40	0.60	0.33	0.70	0.25
	320	1.04	0.83	1.27	0.47	0.66	0.29	0.52	0.44	0.41	0.26	0.32	0.14
	330	1.14	0.80	0.92	0.45	0.64	0.28	0.55	0.37	0.36	0.35	0.36	0.19
	340	1.34	0.93	1.79	0.68	0.72	0.33	0.54	0.42	0.34	0.35	0.46	0.15
	350	1.48	0.94	1.82	0.61	0.69	0.29	0.68	0.42	0.30	0.43	0.52	0.19
	360	1.56	1.15	1.98	0.79	0.70	0.32	0.53	0.42	0.34	0.30	0.40	0.10
	370	1.73	4.80	2.27	2.31	1.19	0.38	0.67	0.44	0.24	0.20	0.40	0.16
	385	1.79	6.03	2.42	1.63	1.82	0.40	0.57	0.43	0.44	0.19	0.35	0.16
	400	2.04	14.86	24.50	5.62	1.86	0.38	0.66	0.47	0.42	0.19	0.41	0.43
	420	2.21	103.64	47.22	24.65	11.05	0.44	0.64	0.60	0.52	0.21	0.38	0.48
	450	2.41	300.18	125.88	95.72	36.94	0.45	0.88	0.90	0.79	0.24	0.37	0.51
#27	Unheated	0.45	0.79	0.48	0.53	0.09	0.47	0.60	0.37	0.27	0.43	0.28	0.16
	230	0.65	0.78	0.63	0.69	0.49	0.41	0.75	0.38	0.39	0.38	0.33	0.16
	280	0.86	0.94	0.69	0.88	0.63	0.43	0.74	0.40	0.34	0.38	0.36	0.11
	310	1.19	0.79	1.11	0.55	0.41	0.37	0.44	0.35	0.18	0.39	0.33	0.22
	320	1.21	0.95	0.65	0.67	0.41	0.34	0.43	0.36	0.20	0.33	0.31	0.23
	330	1.24	1.03	0.27	0.78	0.61	0.34	0.70	0.39	0.13	0.38	0.31	0.24
	340	1.32	1.12	1.32	0.84	0.21	0.36	0.66	0.38	0.18	0.31	0.29	0.10
	350	1.36	1.21	1.70	0.88	0.78	0.31	0.52	0.37	0.22	0.28	0.32	0.16
	360	1.54	1.29	1.84	0.97	0.91	0.36	0.50	0.39	0.21	0.28	0.30	0.14
	370	1.69	3.37	1.73	1.75	0.67	0.33	0.72	0.42	0.33	0.20	0.23	0.09
	385	1.71	4.24	4.02	1.41	1.66	0.38	0.46	0.33	0.36	0.19	0.17	0.17
	400	1.96	14.66	2.74	5.80	1.32	0.40	0.61	0.45	0.29	0.19	0.20	0.45
	420	2.16	100.28	48.09	23.46	10.02	0.43	0.66	0.58	0.50	0.71	0.13	0.51
	450	2.33	199.44	69.43	63.74	45.64	0.48	0.93	0.90	0.79	0.29	0.17	0.50
#V19.13	Unheated	0.51	1.58	0.17	0.99	0.35	0.46	0.45	0.52	0.39	0.42	0.38	0.11
	230	0.55	2.81	0.31	1.90	0.59	0.44	0.40	0.45	0.53	0.38	0.34	0.22
	280	0.80	2.70	0.37	1.65	0.62	0.44	0.40	0.41	0.34	0.40	0.36	0.23
	310	0.98	4.86	1.82	2.90	0.76	0.52	0.41	0.43	0.47	0.44	0.41	0.15
	320	1.09	3.73	3.07	2.94	0.70	0.46	0.52	0.46	0.45	0.37	0.36	0.36
	330	1.18	2.46	2.61	2.05	0.48	0.41	0.62	0.36	0.42	0.31	0.37	0.35
	340	1.27	3.70	5.49	2.93	5.71	0.42	0.51	0.40	0.40	0.32	0.41	0.33

	360	1.49	3.40	5.13	3.05	4.45	0.40	0.43	0.44	0.32	0.28	0.41	0.20
	370	1.55	8.01	1.67	5.29	7.36	0.38	0.52	0.34	0.18	0.24	0.44	0.49
	385	1.61	9.63	10.76	4.24	9.13	0.39	0.55	0.31	0.38	0.24	0.42	0.15
	400	1.96	19.52	31.72	12.29	11.13	0.35	0.56	0.44	0.38	0.23	0.43	0.54
	420	2.10	67.64	81.35	25.25	21.36	0.35	0.62	0.51	0.50	0.19	0.40	0.53
	450	2.32	257.58	93.57	118.80	40.16	0.43	0.89	0.89	0.85	0.43	0.43	0.50
#34	Unheated	0.20	n.a. ¹	n.a.	n.a.	n.a.	n.a.	n.a.	n.a.	n.a.	n.a.	n.a.	n.a.
	230	0.44	0.27	0.28	0.23	0.02	0.20	0.38	0.41	0.43	0.27	0.36	0.10
	250	0.56	0.34	0.69	0.21	0.19	0.36	0.54	0.43	0.60	0.30	0.41	0.09
	280	0.69	0.21	0.21	0.12	0.09	0.35	0.29	0.51	0.50	0.33	0.45	0.19
	310	0.94	0.67	0.42	1.04	0.05	0.20	0.26	0.58	0.51	0.34	0.50	0.20
	340	1.24	1.13	1.09	0.84	0.02	0.34	0.35	0.37	0.42	0.23	0.44	0.25
	370	1.70	3.87	0.96	3.26	0.24	0.26	0.58	0.40	0.27	0.16	0.30	0.23
	400	1.93	1.54	2.26	1.40	0.17	0.31	0.64	0.50	0.41	0.20	0.35	0.46
#35	Unheated	0.20	n.a.	n.a.	n.a.	n.a.	n.a.	n.a.	n.a.	n.a.	n.a.	n.a.	n.a.
	230	0.44	0.54	0.90	0.27	0.42	0.43	0.54	0.34	0.33	0.28	0.35	0.07
	250	0.66	0.65	0.58	0.60	0.40	0.37	0.61	0.46	0.40	0.39	0.33	0.08
	280	0.72	1.14	0.90	0.96	0.33	0.34	0.35	0.47	0.31	0.27	0.31	0.10
	310	0.92	1.36	0.89	1.24	0.15	0.35	0.74	0.30	0.32	0.22	0.26	0.23
	340	1.32	1.53	0.76	1.63	0.19	0.31	0.44	0.41	0.57	0.31	0.36	0.24
	370	1.67	2.44	0.40	2.44	0.45	0.33	0.67	0.40	0.22	0.26	0.39	0.22
	385	1.55	0.77	0.40	0.26	0.04	0.50	0.57	0.26	0.30	0.33	0.54	0.36
	400	1.84	1.19	0.32	0.99	0.58	0.25	0.74	0.50	0.24	0.25	0.43	0.50
	430	1.87	6.55	3.83	3.97	0.67	0.30	0.65	0.59	0.47	0.19	0.30	0.37
	450	2.24	14.25	12.57	8.59	2.31	0.31	0.78	0.88	0.56	0.23	0.28	0.43

^a Diamondoids = ppm 3-+4-methyldiamantane in pyrolysates.

^b Adam = ppm adamantane in pyrolysates.

^c Diam = ppm diamantane in pyrolysates.

^d Triam = ppm triamantane in pyrolysates.

^e MDI = 4-Methyldiamantane/(1-+3-+4-methyldiamantanes).

^f MAI = 1-Methyladamantane/(1-+2-methyladamantanes).

^g EAI = 1-Ethyladamantane/(1-+2-ethyladamantanes).

^h DMAI = 1,3-Dimethyladamantane/(1,2-+1,3-dimethyladamantanes).

ⁱ DMI-1 = 4,9-Dimethyldiamantane/(4,9-+3,4-dimethyldiamantanes).

^j DMI-2 = 4,9-Dimethyldiamantane/(4,9-+4,8-dimethyldiamantanes).

^k MTI = 9-Methyltriamantane/(5-+8-+9-+16-methyltriamantanes).

¹ Not available.

shown in Table 6, there is no significant change in the abundance of diamondoids in the rock and peat pyrolysates below 340 °C. Other diamondoid species, including adamantane, diamantane and triamantane, behave similarly with respect to abundance in the pyrolysates (Fig. 7). However, it is notable that the generation curve of triamantane is different from those of adamantane and diamantane for the Vinini limestone. Greater quantities of triamantane appear to be produced from the Vinini limestone than the Irati samples.

A sharp increase in diamondoid amount in the pyrolysates is generally observed above 360 °C for rocks and above 340 °C for peats (Table 6). This is indicative of intense cracking of liberated hydrocarbons, whereby the less thermally stable hydrocarbons break down to smaller and more stable molecules, such as methane and aromatic hydrocarbons with smaller rings. In contrast, diamondoids are increasingly concentrated because they are highly stable and relatively resistant to thermal degradation. Consequently, oil cracking

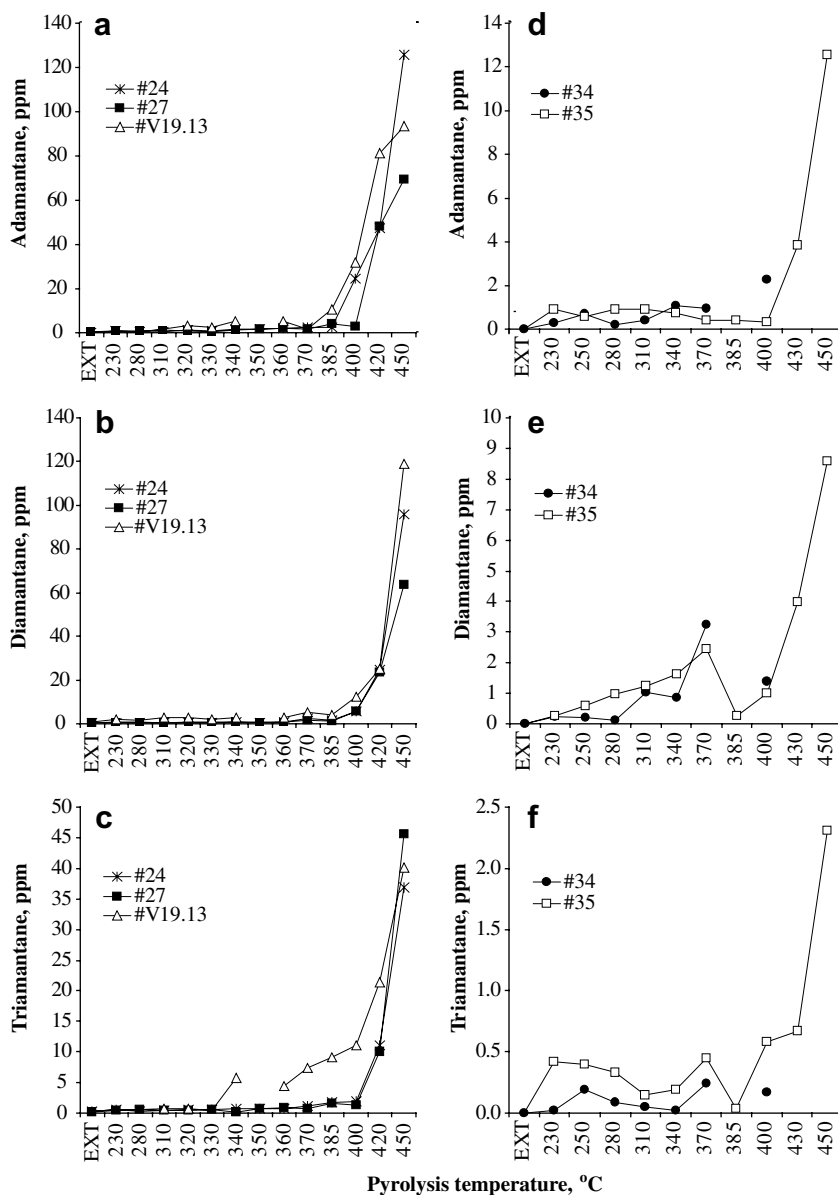


Fig. 7. Concentrations of parent diamondoids (adamantane, diamantane and triamantane) in hydrous pyrolysates from immature source rocks and peats for isothermal experiments at various temperatures. EXT = concentration in extract prior to pyrolysis.

substantially elevates the concentrations of diamondoids in pyrolysate liquids. While their generation still proceeds throughout the oil window, the amount produced decreases at higher temperature ($> 340\text{ }^{\circ}\text{C}$), most likely due to the fact that the acidic clay minerals lose their catalytic activity upon mineral transformation. Hence, the enrichment in diamondoids via destruction of other compounds becomes more important than the generation of diamondoids.

Irrespective of mechanism, the concentrations of diamondoids in pyrolysates increase consistently with increasing pyrolysis temperature ($> 340\text{ }^{\circ}\text{C}$) suggesting that their concentrations in oils can be used as a molecular proxy for thermal maturity. For example, they reach maximum concentrations of 300, 199 and 258 ppm in the pyrolysates of Irati limestone and oil shale, and Vinini limestone, respectively, at $450\text{ }^{\circ}\text{C}$. Although concentrations are significantly lower in the peat pyrolysates, maximum concentration for bog peat occurs in the $450\text{ }^{\circ}\text{C}$ experiment. Curiously, the concentrations do not vary systematically with temperature and decreases are observed at 370 and $400\text{ }^{\circ}\text{C}$ for fen and bog peats, respectively. This phenomenon is not well understood at present.

3.7. Behavior of diamondoid parameters with thermal maturity

The bridgehead-methylated diamondoids are known to be thermodynamically more stable than other methylated diamondoid species (Clark et al., 1979; Appendix A). On this basis, Chen et al. (1996) and Li et al. (2000) studied the maturity of over-mature crude oils and source rocks using 4-MD/(1-+3-+4-MD) (MDI), 1-MA/(1-+2-MA) (MAI), and 1-EA/(1-+2-EA) (EAI) as maturity indicators (refer to Table 6). Zhang et al. (2005) documented other diamondoid-related maturity parameters, e.g., 1,3-DMA/(1,2-+1,3-DMA) (DMAI), 4,9-DMD/(4,9-+3,4-DMD) (DMDI-1), 4,9-DMD/(4,8-+4,9-DMD) (DMDI-2) in a study of Tarim Paleozoic marine oils. However, our results indicate that none of these parameters shows systematic change as heating temperature increases and vitrinite reflectance increases to $R_0 < 1.3\%$ (Table 6). In some cases, a reversal can be observed for some parameters. At higher levels of thermal stress, several ratios, including MDI, MAI, EAI, and DMAI, generally increase with

maturity (Table 6). This implies that these parameters might be useful in the assessment of crude oils and source rocks at high thermal maturity (equivalent to $R_0 > 1.3\%$). Note that the isomerization ratio for methyl triamantanes, 9-MT/(5-+8-+16-MT), shows good correlation with R_0 throughout the temperature range examined (Table 6), indicating that it may be a reliable broad range maturity indicator.

It is possible that more than one factor controls these ratios, distorting their ability to reflect thermal maturity equivalent to $R_0 < 1.3\%$. As a result, the ratios change inconsistently and even in a reverse manner with the respect to increasing maturity. However, at maturity levels equivalent to $R_0 > 1.3\%$, one or more of these competing influences may no longer contribute and the parameters exhibit systematic trends with increasing thermal stress. Alternatively, the conversion of methylated isomers could become more significant at higher maturity ($R_0 > 1.3\%$) than at lower maturity ($R_0 < 1.3\%$), so the isomerization ratios for substituted diamondoids may be more sensitive at $R_0 > 1.3\%$.

3.8. Calibration of diamondoids as a proxy for thermal maturity

Although the diamondoid maturity parameters are usable in maturity assessment to some extent, they have unavoidable limitations. Our results indicate that the absolute concentration can be used as a unique maturity indicator for source rocks and oils, particularly in cases where other maturity data are unavailable. Vitrinite reflectance is a commonly used yardstick for measuring maturity of source rocks (Tissot and Welte, 1984). Therefore, we calibrated the concentration of diamondoids in generated oils with R_0 values measured on the pyrolysis residues. The fitting curves are presented in Fig. 8 and show that the concentration of diamondoids correlates with R_0 at higher maturity levels ($R_0 \geq 1.3\%$), suggesting that the diamondoid abundance is more sensitive at higher levels of thermal stress. The good relationship between concentration and R_0 provides a useful tool for projecting the thermal maturity of either oils or source rocks if the concentration of diamondoids is known. Based on linear regression ($R_0 < 1.3\%$) and exponential regression ($R_0 \geq 1.3\%$; Fig. 8), equations showing the relationships can be established using hydrous

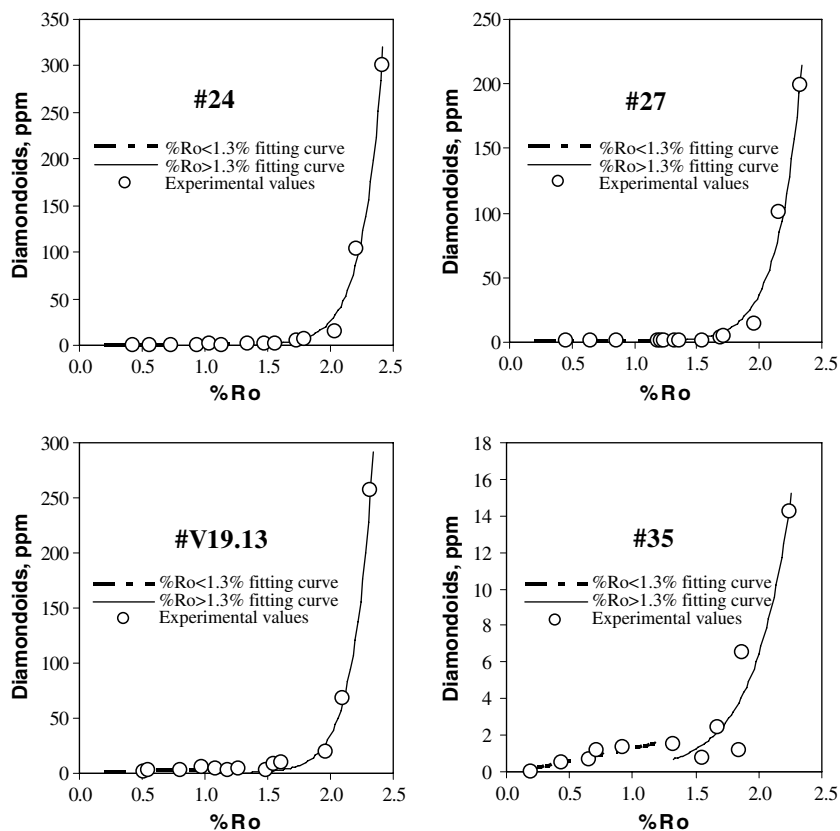


Fig. 8. Total diamondoid concentration in hydrous pyrolysates and R_0 measured on pyrolysis residues showing increasing abundance of diamondoids with thermal maturity during evolution of organic matter in source rocks and peats.

pyrolysis data. For Irati limestone, the following relationships are obtained:

$$C_{\text{diamondoids}} = 0.0001622 \cdot e^{5.99 \cdot R_0}$$

$$r^2 = 0.9937 (R_0 \geq 1.3\%)$$

$$C_{\text{diamondoids}} = 0.6384 \cdot R_0 + 0.0853$$

$$r^2 = 0.7600 (R_0 < 1.3\%)$$

where $C_{\text{diamondoids}}$ is the concentration of diamondoids (3-+4-methyldiamantanes) in hydrous pyrolysates at any maturity level. Similarly, the concentration in the hydrous pyrolysates of Irati oil shale is calibrated with R_0 as follows:

$$C_{\text{diamondoids}} = 0.00127 \cdot e^{5.143 \cdot R_0},$$

$$r^2 = 0.9854 (R_0 \geq 1.3\%),$$

$$C_{\text{diamondoids}} = 0.2757 \cdot R_0 + 0.06415,$$

$$r^2 = 0.4910 (R_0 < 1.3\%).$$

For Vinini limestone, the relationships are:

$$C_{\text{diamondoids}} = 0.0001176 \cdot e^{6.293 \cdot R_0},$$

$$r^2 = 0.9970 (R_0 \geq 1.3\%),$$

$$C_{\text{diamondoids}} = 1.9082 \cdot R_0 + 1.3807,$$

$$r^2 = 0.2888 (R_0 < 1.3\%).$$

With respect to the bog peat, they are:

$$C_{\text{diamondoids}} = 0.008287 \cdot e^{3.327 \cdot R_0},$$

$$r^2 = 0.9007 (R_0 \geq 1.3\%),$$

$$C_{\text{diamondoids}} = 1.3966 \cdot R_0 - 0.1216,$$

$$r^2 = 0.8823 (R_0 < 1.3\%).$$

Any improvement in these correlations would require more extensive data at both low and high R_0 levels. Vitrinite is usually absent from Paleozoic carbonate source rocks, which makes it difficult to determine their maturity. Therefore, diamondoids can be a useful molecular indicator in the assessment of mature to highly mature Paleozoic carbonates.

Table 7

The extent of oil cracking estimated from concentration of diamondoids in hydrous pyrolysates of immature rocks and peats

Sample no.	R_0 (%)	Diamondoids (ppm)	$R_0 \geq 1.1\%$		$R_0 \geq 1.2\%$		$R_0 \geq 1.3\%$	
			C_0^a (ppm)	Cracking (%)	C_0 (ppm)	Cracking (%)	C_0 (ppm)	Cracking (%)
#24	0.43	0.34	0.56	–	0.60	–	0.60	–
	0.56	0.36	–	–	–	–	–	–
	0.73	0.76	–	–	–	–	–	–
	0.94	0.52	–	–	–	–	–	–
	1.04	0.83	–	–	–	–	–	–
	1.14	0.80	–	29.75	–	–	–	–
	1.34	0.93	–	39.57	–	35.30	–	35.30
	1.48	0.94	–	40.21	–	35.99	–	35.99
	1.56	1.15	–	51.13	–	47.68	–	47.68
	1.73	4.80	–	88.29	–	87.47	–	87.47
	1.79	6.03	–	90.68	–	90.02	–	90.02
	2.04	14.86	–	96.22	–	95.95	–	95.95
	2.21	103.64	–	99.46	–	99.42	–	99.42
2.41	300.18	–	99.81	–	99.80	–	99.80	
#27	0.45	0.79	0.84	–	0.83	–	0.88	–
	0.65	0.78	–	–	–	–	–	–
	0.86	0.94	–	–	–	–	–	–
	1.19	0.79	–	–	–	–	–	–
	1.21	0.95	–	11.93	–	13.16	–	–
	1.24	1.03	–	18.77	–	19.90	–	–
	1.32	1.12	–	25.29	–	26.34	–	21.43
	1.36	1.21	–	30.85	–	31.82	–	27.27
	1.54	1.29	–	35.14	–	36.05	–	31.78
	1.69	3.37	–	75.17	–	75.52	–	73.89
	1.71	4.24	–	80.27	–	80.54	–	79.25
	1.96	14.66	–	94.29	–	94.37	–	94.00
	2.16	100.28	–	99.17	–	99.18	–	99.12
2.33	199.44	–	99.58	–	99.59	–	99.56	
#V19.13	0.51	1.58	3.14	–	3.02	–	3.12	–
	0.55	2.81	–	–	–	–	–	–
	0.8	2.70	–	–	–	–	–	–
	0.98	4.86	–	–	–	–	–	–
	1.09	3.73	–	–	–	–	–	–
	1.18	2.46	–	–	–	–	–	–
	1.27	3.70	–	10.38	–	18.29	–	–
	1.49	3.40	–	2.47	–	11.08	–	8.24
	1.55	8.01	–	58.60	–	62.26	–	61.05
	1.61	9.63	–	65.57	–	68.61	–	67.60
	1.96	19.52	–	83.01	–	84.51	–	84.02
	2.1	67.64	–	95.10	–	95.53	–	95.39
	2.32	257.58	–	98.71	–	98.83	–	98.79
#34	0.20	0	0.30	–	0.30	–	0.44	–
	0.44	0.27	–	–	–	–	–	–
	0.56	0.34	–	–	–	–	–	–
	0.69	0.21	–	–	–	–	–	–
	0.94	0.67	–	–	–	–	–	–
	1.24	1.13	–	73.63	–	73.63	–	–
	1.70	3.87	–	92.30	–	92.30	–	88.72
	1.93	1.54	–	80.65	–	80.65	–	71.65
#35	0.20	0	0.74	–	0.74	–	0.74	–
	0.44	0.54	–	–	–	–	–	–
	0.66	0.65	–	–	–	–	–	–

(continued on next page)

Table 7 (continued)

Sample no.	R_0 (%)	Diamondoids (ppm)	$R_0 \geq 1.1\%$		$R_0 \geq 1.2\%$		$R_0 \geq 1.3\%$	
			C_0^a (ppm)	Cracking (%)	C_0 (ppm)	Cracking (%)	C_0 (ppm)	Cracking (%)
	0.72	1.14	–	–	–	–	–	–
	0.92	1.36	–	–	–	–	–	–
	1.32	1.53	51.76	51.76	51.76	51.76	51.76	51.76
	1.67	2.44	69.75	69.75	69.75	69.75	69.75	69.75
	1.55	0.77	4.16	4.16	4.16	4.16	4.16	4.16
	1.84	1.19	37.98	37.98	37.98	37.98	37.98	37.98
	1.87	6.55	88.73	88.73	88.73	88.73	88.73	88.73
	2.24	14.25	94.82	94.82	94.82	94.82	94.82	94.82

Note: The extent of oil cracking was calculated according to the method reported by Dahl et al. (1999).

^a C_0 is the concentration of diamondoids (3-+4-methyldiamantanes) in the uncracked hydrous pyrolysates (“diamondoid baseline”). It corresponds to the average concentration of diamondoids in pyrolysates at maturity levels of $R_0 < 1.1\%$, or 1.2% , or 1.3% .

4. Diamondoids as a molecular proxy for oil cracking

Diamondoids are progressively enriched in oils as other less stable compounds are cracked. In some cases, where the petroleum liquids have experienced extreme temperature in either reservoir or source rock, the oil is completely dominated by diamondoid species, as evidenced by the condensates from the Deep Norphlet Trend in the Gulf of Mexico (Dahl et al., 2000). Another possible mechanism for the concentration change in oil is thermochemical sulfate reduction (TSR), which can destroy other hydrocarbons in deep hot petroleum reservoirs (e.g., Orr, 1974; Krouse et al., 1988). The effect of TSR on the diamondoid concentration is, however, negligible since only extremely low amounts (< 1%) can be altered by the TSR process (Wei et al., personal communication). Thus, the extent of oil cracking can be estimated on the basis of diamondoid concentration.

According to the method developed by Dahl et al. (1999), the extent of oil cracking is expressed as:

$$\% \text{ cracking} = (1 - C_0/C_c) \times 100,$$

where C_0 is the concentration of diamondoids (3-+4-methyldiamantanes) in the non-cracked pyrolysate (also called “diamondoid baseline”) and C_c is the concentration of diamondoids in the cracked pyrolysate at any maturity level. The diamondoid baseline (C_0) here is determined by the average concentration in pyrolysates prior to cracking in order to minimize the variation in concentration. Assuming that the beginning of oil cracking is at about $R_0 = 1.1\%$, the baselines are calculated as 0.56,

0.84, 3.14, 0.30 and 0.74 ppm for Irati limestone and oil shale, Vinini limestone, and Germany fen and bog peats, respectively (Table 7). Therefore, we can determine that 29.75% of hydrocarbons have undergone cracking at $R_0 = 1.14\%$ for Irati limestone during hydrous pyrolysis, consistent with the assumption that thermal breakdown of petroleum hydrocarbons occurs around $R_0 = 1.1\%$. Likewise, we can obtain the extent of oil cracking for Irati oil shale, Vinini limestone and bog peat, which is 11.93% at $R_0 = 1.21\%$, 10.38% at $R_0 = 1.27\%$, and 51.76% at $R_0 = 1.32\%$, respectively. Only minor differences are observed in the cracking percentages using the diamondoid baselines assuming that oil cracking starts either at $R_0 = 1.2\%$ or at $R_0 = 1.3\%$ (Table 7). Hence, for a given source rock or oil, we can use diamondoid concentration to determine the extent of cracking based on the cracking formula, as well as the thermal maturity using the diamondoid- R_0 equations derived above.

As suggested by Dahl et al. (1999), the diamondoid method may overestimate the extent of oil cracking, especially for highly cracked samples due to evaporative loss of light ends from oils or rock extracts during the experimental workup procedure. This may also have occurred in the pyrolysate products in this study where the extent of pyrolysate cracking may be overestimated. Even so, the diamondoid-oil cracking approach is believed to be more accurate than the GOR (gas-to-oil ratio) method for predicting the extent of oil cracking because numerous processes can contribute to GOR such as migration, gas leakage and biodegradation (e.g., Claypool and Mancini, 1989; Welte et al., 1997).

5. Conclusions

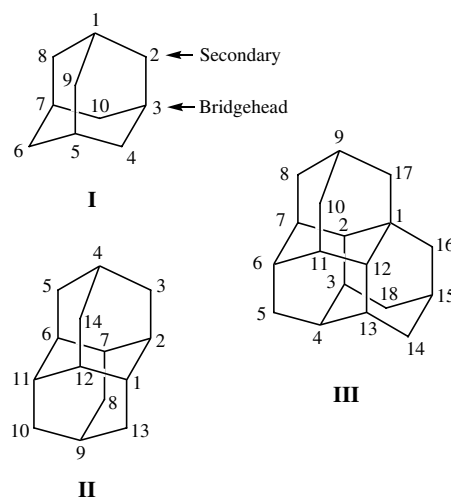
- (1) The generation of oils from hydrous pyrolysis of immature rocks and peats maximizes at temperatures ranging from 340 to 360 °C depending on lithology and type of organic matter.
- (2) Biomarker maturity parameters show non-systematic changes with increasing thermal stress in these hydrous pyrolysis experiments. Biomarkers are greatly reduced in rock and peat pyrolysates at higher temperatures (> 370 °C) because of intense thermal cracking.
- (3) The formation of diamondoids begins prior to oil generation in some sedimentary rocks. They can be generated from the artificial maturation of immature rocks and peats. Their concentration increases significantly above temperatures of 360–370 °C (equivalent $R_0 = 1.3$ – 1.5%) due to intense oil cracking and successive creation of diamondoids. Diamondoids are generated in pyrolysates of peat samples, but their concentrations remain relatively low and appear to decrease at ~ 370 °C before increasing at the highest pyrolysate temperatures.
- (4) Diamondoid maturity parameters based on isomer stability may not be useful below R_0 1.3%, as indicated by significant variability in hydrous pyrolysis experiments. They appear to behave more systematically at $R_0 \geq 1.3\%$.
- (5) Differences are observed in the abundance of diamondoids in extracts of unheated sedimentary rocks. These differences may be a result of subtle maturity differences, variations in organic matter input, and/or the distinct mineralogy of each rock type.
- (6) The established relationships between the concentrations of diamondoids in rock and peat pyrolysates and R_0 can be used to determine the thermal maturity of either source rocks or crude oils and help understand thermal evolution of petroleum if concentrations of diamondoids are known.
- (7) Diamondoids can serve as a molecular proxy for estimating extent of oil cracking.

Acknowledgements

We appreciate the valuable discussion with Jeremy Dahl and Mike Lewan regarding the possible

sources of diamondoids and hydrous pyrolysis. We thank Jianqi Tu for measuring the vitrinite reflectance of some rocks and peats from hydrous pyrolysis experiments. Yongshe Liu helped work out the fitting equations for different types of source rocks and peats using Matlab software. We thank Steve Jacobson for providing the Vinini Creek rock sample and Jürgen Rullkötter for the German peat samples. We are very grateful to Cara Davis and Robert Kagi for insightful comments and suggestions which greatly improved the manuscript. The study was supported by Molecular Organic Geochemistry Industrial Affiliates (MOGIA) and McGee funds at Stanford University.

Appendix A



Associate Editor—Clifford C. Walters

References

- Albrecht, P., Vandenbroucke, M., Mandengue, M., 1976. Geochemical studies on the organic matter from the Douala Basin (Cameroon). I. Evolution of the extractable organic matter and the formation of petroleum. *Geochimica et Cosmochimica Acta* 40, 791–799.
- Brown, D.R., Rhodes, C.N., 1997. Brønsted and Lewis acid catalysis with ion-exchanged clays. *Catalysis Letters* 45, 35–40.
- Chen, J., Fu, J., Sheng, G., Liu, D., Zhang, J., 1996. Diamondoid hydrocarbon ratios: novel maturity indices for highly mature crude oils. *Organic Geochemistry* 25, 179–190.
- Chung, H.M., Walters, C.C., Bucks, S., Bingham, G., 1998. Mixed signals of the source and thermal maturity for petroleum accumulations from light hydrocarbons: an example of the Beryl Field. *Organic Geochemistry* 29, 381–396.

- Clark, T., Knox, T.M., McKervey, M.A., Mackle, H., Rooney, J.J., 1979. Thermochemistry of bridgehead-ring substances. Enthalpies of formation of some diamondoid hydrocarbons and perhydroquinacene-comparisons with data from empirical force field calculations. *Journal of American Chemical Society* 101, 2404–2410.
- Claypool, G.E., Mancini, E.A., 1989. Geochemical relationships of petroleum in Mesozoic reservoirs to carbonate source rocks of Jurassic Smackover Formation, South west Alabama. *American Association of Petroleum Geologists Bulletin* 73, 904–924.
- Connan, J., 1974. Diagenese naturelle et diagenese artificielle de la matiere organique a element vegetaux predominants. In: Tissot, B.P., Biener, F. (Eds.), *Advances in Organic Geochemistry 1973*. Éditions Technip, Paris, pp. 73–95.
- Cseri, T., Bekassy, S., Figueras, F., Rizner, S., 1995. Benzylolation of aromatics on ion-exchanged clays. *Journal of Molecular Catalysis A* 98, 101–107.
- Czochanska, A., Gilbert, T.D., Philp, R.P., Sherppard, C.M., Weston, R.J., Wood, T.A., Woolhouse, A.D., 1988. Geochemical application of sterane and triterpane biomarkers to a description of oils from the Taranaki Basin in New Zealand. *Organic Geochemistry* 12, 123–135.
- Dahl, J.E., Moldowan, J.M., Lipton, P.A., 2000. Diamondoids as source indicators. *Molecular Organic Geochemistry Industrial Affiliates, Stanford University, Workshop, Internal Report*.
- Dahl, J.E., Moldowan, J.M., Peters, K., Claypool, G., Rooney, M., Michael, G., Mellos, M., Kohnen, M., 1999. Diamondoid hydrocarbons as indicators of oil cracking. *Nature* 399, 54–56.
- Dahl, J.E., Moldowan, J.M., Peters, K.E., Mello, M.R., 1998. Diamondoid hydrocarbons as indicators of thermal maturity and oil-cracking. Abstract, *American Association of Petroleum Geologists Bulletin* 82, 1883–1984.
- Eberl, D., 2003. User's guide to RockJock – A program for determining quantitative mineralogy from powder X-ray diffraction data. *United States Geological Survey Open-File Report 03-78*, p. 42.
- Fort, R.C., 1976. Rearrangements leading to adamantanes. In: *Adamantane: The Chemistry of Diamond Molecules*. Marcel Dekker, Inc., pp. 35–66.
- Fu, J., Sheng, G., Peng, P., Brassell, S.C., Eglinton, G., Jiang, J., 1986. Peculiarities of salt lake sediments as potential source rocks in China. *Organic Geochemistry* 10, 119–126.
- Huizinga, B.J., Tannenbaum, E., Kaplan, I.R., 1987a. The role of minerals in the thermal alteration of organic matter-III. Generation of bitumen in laboratory experiments. *Organic Geochemistry* 11, 591–604.
- Huizinga, B.J., Tannenbaum, E., Kaplan, I.R., 1987b. The role of minerals in the thermal alteration of organic matter-IV. Generation of *n*-alkanes, acyclic isoprenoids, and alkenes in laboratory experiments. *Geochimica et Cosmochimica Acta* 51, 1083–1097.
- Hunt, J.M., Whelan, J.K., Huc, A.Y., 1980. Genesis of petroleum hydrocarbons in marine sediments. *Science* 209, 403–404.
- Krouse, H.R., Viau, C.A., Eliuk, L.S., Ueda, A., Halas, S., 1988. Chemical and isotopic evidence of thermochemical sulfate reduction by light hydrocarbon gases in deep carbonate reservoirs. *Nature* 333, 415–419.
- Lewan, M.D., 1993. Laboratory simulation of petroleum formation-hydrous pyrolysis. In: Engel, M.H., Macko, S.A. (Eds.), *Organic Geochemistry, Principles and Applications*. Plenum Press, New York, pp. 419–444.
- Li, J., Philp, P., Cui, M., 2000. Methyl diamantane index (MDI) as a maturity parameter for Lower Paleozoic carbonate rocks at high maturity and overmaturity. *Organic Geochemistry* 31, 267–272.
- Mackenzie, A.S., Patience, R.L., Maxwell, J.R., Vandenbroucke, M., Durand, B., 1980. Molecular parameters of maturation in the Toarcian shales, Paris Basin, France – I. Changes in the configuration of acyclic isoprenoid alkanes, steranes, and triterpanes. *Geochimica et Cosmochimica Acta* 44, 1709–1721.
- Moldowan, J.M., Seifert, W.K., Gallegos, E.J., 1985. Relationship between petroleum composition and depositional environment of petroleum source rocks. *American Association of Petroleum Geologists Bulletin* 69, 1255–1268.
- Moldowan, J.M., Fago, F.J., Lee, C.Y., Jacobson, S.R., Watt, D.S., Slogui, N.E., Jeganathan, A., Young, D.C., 1990. Sedimentary 24-*n*-propylcholestanes, molecular fossils diagnostic of marine algae. *Science* 247, 309–312.
- Moldowan, J.M., Fago, F.J., Carlson, R.M.K., Young, D.C., Duynne, G.V., Clardy, J., Schoell, M., Pillinger, C.T., Watt, D.S., 1991. Rearranged hopanes in sediments and petroleum. *Geochimica et Cosmochimica Acta* 55, 3333–3353.
- Orr, W.L., 1974. Changes in sulfur content and isotopic ratios of sulfur during petroleum maturation-study of Big Horn Basin Paleozoic oils. *American Association of Petroleum Geologists Bulletin* 58, 2295–2318.
- Ouirisson, G., Alberecht, P., Rohmer, M., 1982. Predictive microbial biochemistry from molecular fossils to prokterotic membranes. *Trends in Biochemical Sciences* 7, 236–239.
- Peters, K.E., Walters, C.C., Moldowan, J.M., 2005. *The Biomarker Guide, Volumes 1 & 2, Biomarkers and Isotopes in Petroleum Exploration and Earth History*. The University Press, Cambridge, 1155pp.
- Petrov, A., Arefjev, D.A., Yakubson, Z.V., 1974. Hydrocarbons of adamantane series as indices of petroleum catagenesis process. In: Tissot, B., Biener, F. (Eds.), *Advances in Organic Geochemistry 1973*. Éditions Technip, Paris, pp. 517–522.
- Radke, M., Schaefer, R.G., Leythaeuser, D., Teichmuller, M., 1980. Composition of soluble organic matter in coals: relation to rank and liptinite fluorescence. *Geochimica et Cosmochimica Acta* 44, 1787–1800.
- Schoell, M., Teschner, M., Wehner, H., Durand, B., Oudin, J.L., 1983. Maturity related biomarker and stable isotope variations and their application to oil/source rock correlation in the Mahakam Delta, Kalimantan. In: Bjorøy, M. et al. (Eds.), *Advances in Organic Geochemistry 1981*. Wiley, New York, pp. 156–163.
- Seifert, W.K., Moldowan, J.M., 1980. The effect of thermal stress on source-rock quality as measured by hopane stereochemistry. *Physics and Chemistry of the Earth* 12, 229–237.
- Tannenbaum, E., Kaplan, I.R., 1985. Role of minerals in the thermal alteration of organic matter I. Generation of gases and condensates under dry conditions. *Geochimica et Cosmochimica Acta* 49, 2589–2604.
- Thompson, K.F.M., 1983. Classification and thermal history of petroleum based on light hydrocarbons. *Geochimica et Cosmochimica Acta* 47, 303–316.
- Tissot, B.P., Welte, D.H., 1984. *Petroleum Formation and Occurrence*, second ed. Springer, New York, pp. 699.

- Volkman, J.K., 1986. A review of sterol markers for marine and terrigenous organic matter. *Organic Geochemistry* 9, 84–99.
- Wei, Z., Zhang, D., Zhang, C., Chen, J., 2001. Study on methylbenzothiophene distribution index as a tool for maturity assessment of source rocks. *Geochimica* 30, 242–247 (in Chinese).
- Wei, Z., Moldowan, J.M., Dahl, J., 2005a. The catalytic effects of minerals on the formation of diamondoids during kerogen pyrolysis. In: 22nd International Meeting of Organic Geochemists (IMOG), Seville, Spain, Abstracts Book Part 1, pp. 260–261.
- Wei, Z., Moldowan, J.M., Dahl, J., 2005b. Formation of diamondoids from hydrous pyrolysis and their potential in modeling oil and gas generation. Stanford Molecular Organic Geochemistry Industrial Affiliates, Internal Report.
- Wei, Z., Moldowan, J.M., Dahl, J., Goldstein, T., Jarvie, D., 2007. The catalytic effects of minerals on the formation of diamondoids from kerogen macromolecules. *Organic Geochemistry* (in press).
- Wei, Z., Moldowan, J.M., Paytan, A., 2006a. Diamondoids and molecular biomarkers generated from modern sediments in the absence and presence of minerals during hydrous pyrolysis. *Organic Geochemistry* 37, 891–911.
- Wei, Z., 2006b. Molecular organic geochemistry of cage compounds and biomarkers in the geosphere: a novel approach to understand petroleum evolution and alteration. Ph.D thesis, Stanford University, pp. 395.
- Welte, D.H., Horfield, B., Barker, D.R., 1997. Petroleum and Basin Evolution. Springer, New York, 535p.
- Wollrab, V., Streibl, M., 1969. Earth waxes, peat, montan wax and other organic brown coal constituents. In: Eglinton, G., Murphy, M.T.J. (Eds.), *Organic Geochemistry – Methods and Results*. Springer, New York, pp. 576–598.
- Zhang, S., Huang, H., Xiao, Z., Liang, D., 2005. Geochemistry of Paleozoic marine petroleum from the Tarim Basin, NW China. Part 2: Maturity assessment. *Organic Geochemistry* 36, 1215–1225.